iScience, Volume *25*

Supplemental information

Dissection of the MEF2D-IRF8 transcriptional circuit dependency in acute myeloid leukemia

Bianca Y. Pingul, Hua Huang, Qingzhou Chen, Fatemeh Alikarami, Zhen Zhang, Jun Qi, Kathrin M. Bernt, Shelley L. Berger, Zhendong Cao, and Junwei Shi

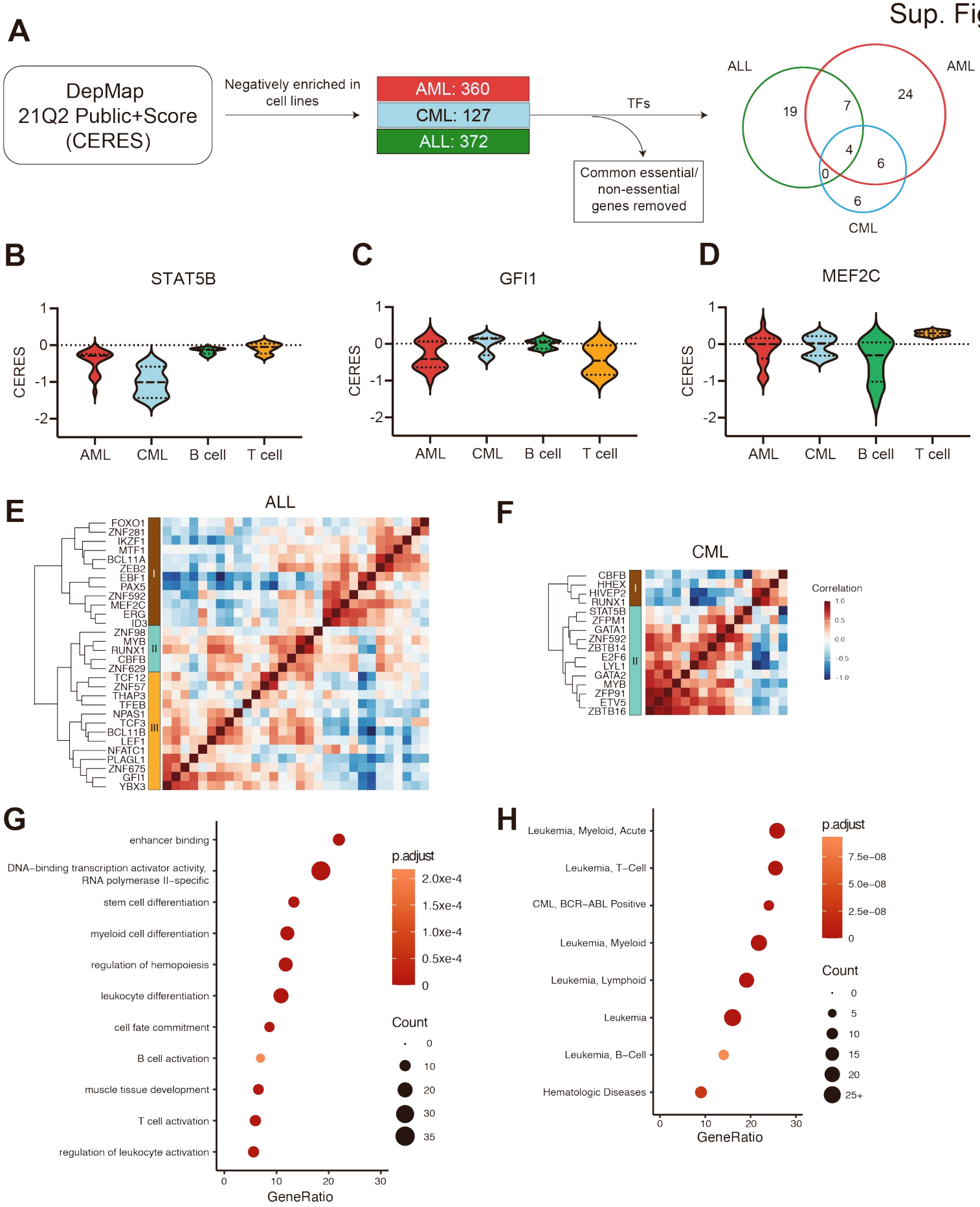

Figure S1. Integrative analysis of TF dependency map in leukemia. Related to Figure 1.
(A) Data analysis workflow. Dependency scores CERES were retrieved from Depmap, and 360, 127, 372 negatively enriched dependencies were found in AML, CML and ALL, respectively. Common essential and non-essential genes were removed, and genes containing DNA-binding domains were used for further analysis. (B-D) Additional violin plots of representative TF CERES effects. (E) Pearson correlation matrix of CERES effects of ALL-biased dependencies among all ALL cell lines. (F) Pearson correlation matrix of CERES effects of CML-biased dependencies among all CML cell lines. (G) Gene Ontology (GO) analysis of the 66 enriched TFs using WebGestalt. (H) Over-Representation Analysis (ORA) of 66 enriched TFs with disease_GLAD4U dataset.

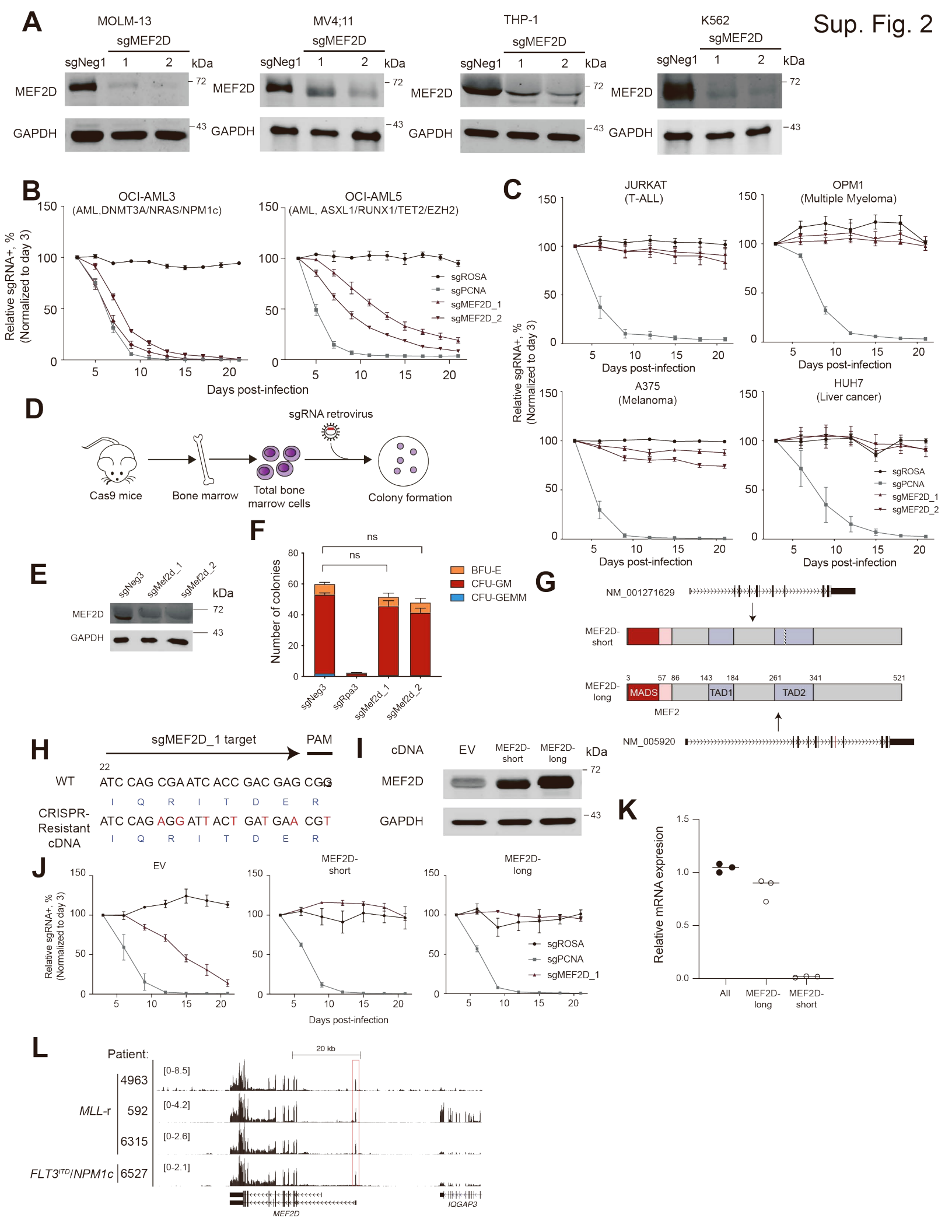
Sup. Fig. 2
A
MOLM-13
MV4;11
THP-1
K562
sgMEF2D
sgNeg1
1
2
kDa
MEF2D
GAPDH
72
43
B
OCI-AML3
(AML,DNMT3A/NRAS/NPM1c)
OCI-AML5
(AML, ASXL1/RUNX1/TET2/EZH2)
Relative sgRNA+, %
(Normalized to day 3)
Days post-infection
sgROSA
sgPCNA
sgMEF2D_1
sgMEF2D_2
C
JURKAT
(T-ALL)
OPM1
(Multiple Myeloma)
A375
(Melanoma)
HUH7
(Liver cancer)
D
sgRNA retrovirus
Cas9 mice
Bone marrow
Total bone
marrow cells
Colony formation
E
sgNeg3
sgMef2d_1
sgMef2d_2
F
ns
Number of colonies
BFU-E
CFU-GM
CFU-GEMM
sgRpa3
G
NM_001271629
MEF2D-
short
MEF2D-
long
MADS
TAD1
TAD2
MEF2
NM_005920
H
sgMEF2D_1 target
PAM
WT
ATC CAG CGA ATC ACC GAC GAG CGG
CRISPR-
Resistant
cDNA
ATC CAG AGG ATT ACT GAT GAA CGT
I Q R I T D E R
I
cDNA
EV
MEF2D-
short
MEF2D-
long
J
EV
MEF2D-
short
MEF2D-
long
K
Relative mRNA expresion
All
L
Patient:
4963
MLL-r
592
6315
FLT3ITD/NPM1c
6527
20 kb
[0-8.5]
[0-4.2]
[0-2.6]
[0-2.1]
MEF2D
IQGAP3

Figure S2. MEF2D is an AML-biased dependency. Related to Figure 2.

(A) Immunoblotting of MEF2D in MOLM-13 (AML, upper left), MV4-11 (AML, upper right), THP-1 (AML, bottom left) and K562 (an acute (erythro)blastic transformation of prior CML, bottom right) cells. (B) Competition-based proliferation assays in OCI-AML3 (AML, left) and OCI-AML5 (AML, right) cells (n=3-5, mean ± SEM). (C) Competition-based proliferation assays in MEF2D-insensitive cells, including JURKAT (T-ALL, n = 3), OPM1 (multiple myeloma, n = 2-3), A375 (melanoma, n = 4) and HUH7 (Liver cancer, n = 4-6) cell lines (mean ± SEM). (D) Schematic of murine bone marrow (BM) colony formation assay. (E) Immunoblotting of MEF2D in whole lysates of BM cells transduced with indicated sgRNAs. (F) Colony formation of Cas9-expressing normal myeloid progenitor cells (n=3). Two-way ANOVA test was performed for statistical analysis. (G) Structure of two human MEF2D isoforms and protein domains (PMID: 29879430). Two isoforms are transcribed from different Transcription Start Site (TSS), and the short isoform (NM_001271629) skips one exon (labeled in red) and loses 7 amino acids of the TAD2 domain. Except that, the encoded proteins for these two isoforms are identical. MADS, MCM1, AGAMOUS, DEFICIENS and SRF domain. TAD, trans-activation domain. (H) Design of CRISPR-resistant MEF2D cDNA. Encoded amino acids are labeled in blue. (I) Immunoblotting of MEF2D in whole-cell lysates of THP-1 cells transduced with Empty Vector (EV), MEF2D-short or -long cDNA. (J) Competition-based proliferation assays in THP-1 cells stably expressing EV or MEF2D cDNA (n=3, mean ± SEM). (K) Reverse transcription-polymerase chain reaction (RT-PCR) indicating relative proportion of the indicated transcripts to total MEF2D transcripts, normalized to GAPDH level (n=3, mean ± SEM). (L) UCSC browser tracks of RNA-seq in human primary AML cells, with the key oncogenic mutations labeled on the left. The transcription start site of the MEF2D-long-unique exon was marked by a red box.

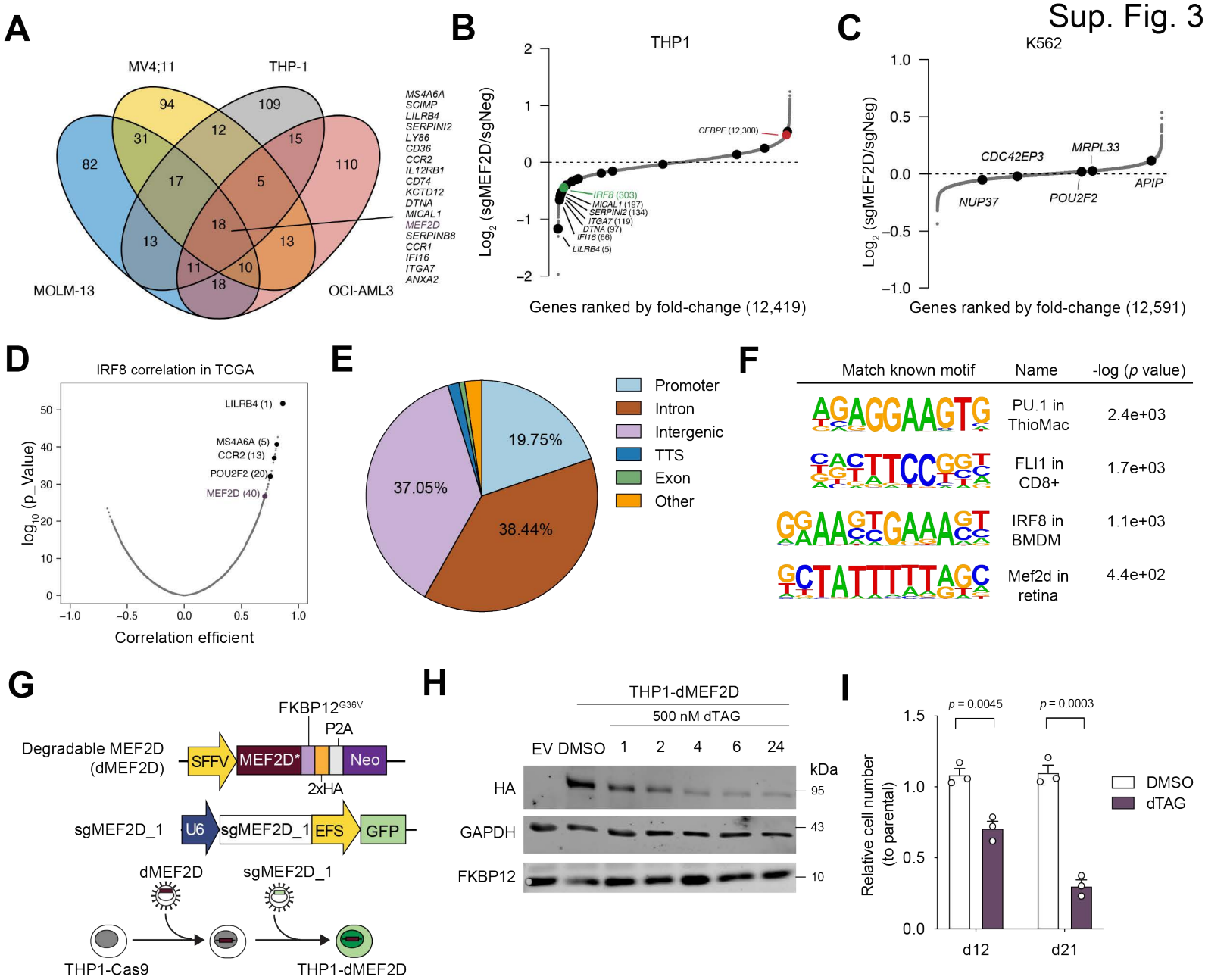

Figure S3. MEF2D-IRF8 regulatory loop in AML. Related to Figure 3. (A) Venn diagram displaying top 200 downregulated gene overlaps upon IRF8 CRISPR-KO between MOLM-13, MV4;11, THP-1 and OCI-AML3 cells (Cao et al., 2021). (B-C) RNA-seq rank plot of gene expression changes in THP-1 (B) or K562 (C) cells 4 days after transduction of two independent sgNeg or sgMEF2D. Dark dots indicate IRF8-regulated genes in Figure S3A. (D) Pearson correlation analysis of IRF8 mRNA expression with other genes in 173 AML patients. (E) Pie chart annotating the distribution of 27,198 MEF2D CUT&RUN peaks in MOLM-13 cells. TTS, transcription termination site. Other, UTR and non-coding RNA regions. (F) MEF2D CUT&RUN-derived known motif analysis in MOLM-13 using HOMER. Shown are known TF motifs. Statistical analysis (p value) was calculated using a binomial test. (G) Schematic describing the establishment of an inducible MEF2D degradation system in THP-1 cells. (H) Immunoblotting of HA, GAPDH and FKBP12 in whole-cell lysates of THP1-dMEF2D cells treated with dTAG-47 in escalated time points. (I) dTAG treatment impaired THP1C-dMEF2D cell growth. Relative cell number of THP1-dMEF2D and parental cells were measured on 12 days and 21 days treatment of DMSO (control) or 500nM dTAG-47 (n=3, mean ± SEM, Student's t-test). (J) RT-qPCR analysis of IRF8, FLT3 and MYC mRNA expression upon 4- and 7-hour 500nM dTAG-47 treatment (normalized to GAPDH, n=3, mean ± SEM, Student's t-test).

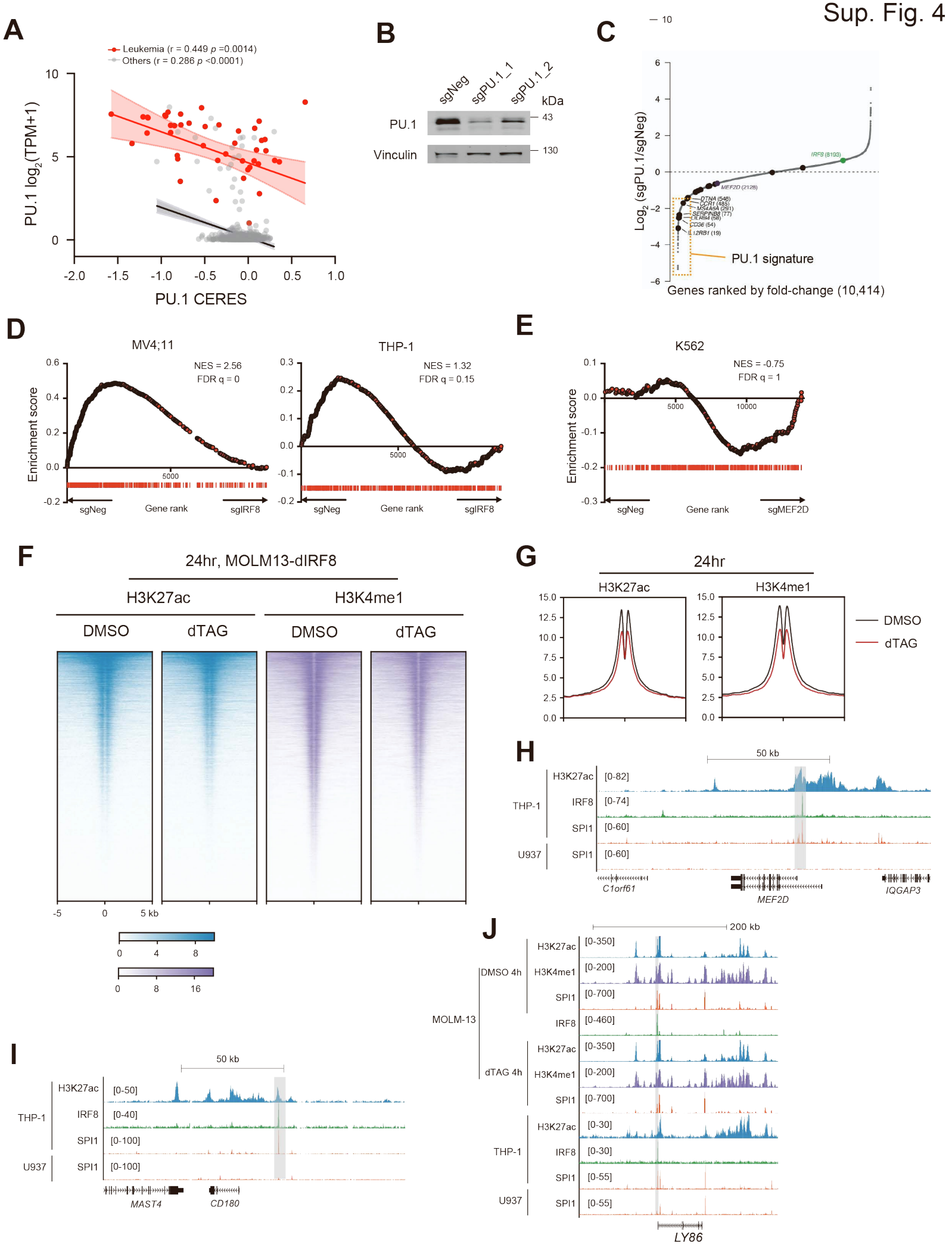
A
Leukemia (r = 0.449 p =0.0014)
Others (r = 0.286 p <0.0001)
PU.1 log2(TPM+1)
PU.1 CERES
B
sgNeg
sgPU.1_1
sgPU.1_2
kDa
PU.1
Vinculin
43
130
C
Log2 (sgPU.1/sgNeg)
Genes ranked by fold-change (10,414)
PU.1 signature
IRF8 (8193)
MEF2D (2128)
D
MV4;11
THP-1
NES = 2.56
FDR q = 0
NES = 1.32
FDR q = 0.15
Enrichment score
sgNeg
Gene rank
sgIRF8
E
K562
NES = -0.75
FDR q = 1
sgMEF2D
F
24hr, MOLM13-dIRF8
H3K27ac
H3K4me1
DMSO
dTAG
-5
0
5 kb
G
24hr
H3K27ac
H3K4me1
DMSO
dTAG
H
50 kb
THP-1
U937
IRF8
SPI1
C1orf61
MEF2D
IQGAP3
I
50 kb
MAST4
CD180
J
200 kb
DMSO 4h
dTAG 4h
MOLM-13
LY86

Figure S4. IRF8 supports PU.1's chromatin occupancy and transcriptional output. Related to Figure 4.
(A) Scatter plot of PU.1 CERES vs mRNA expression in leukemia (red) or other cancer lines from DepMap. PU.1 signature was defined as the top 500 downregulated genes (labeled in the dashed box) and listed in Table S1. (B) Immunoblotting of PU.1 in MOLM-13 whole cell lysates. (C) RNA-seq rank plot of gene expression changes in MOLM-13 cells 5 days after transduction of two independent sgNeg or sgPU.1. (D) GSEA analysis of IRF8-KO RNA-seq data (Cao et al., 2021) in MV4;11 and THP-1 cells. (E) GSEA analysis of MEF2D-KO RNA-seq data in K562 cells. (F-G) Density plot (F) and meta-profiles (G) of H3K27ac and H3K4me1 ChIP-seq signals at IRF8 binding sites in MOLM13-dIRF8 cells upon 24-hour treatment of DMSO or dTAG. (H-I) Gene tracks of H3K27ac, IRF8, PU.1 ChIP-seq signals in THP-1 or U937 cells at MEF2D (H) or CD180 (I) locus.(J) Gene tracks of ChIP-seq signal from Figure 4C-D at LY86 locus.

Sup. Fig. 5

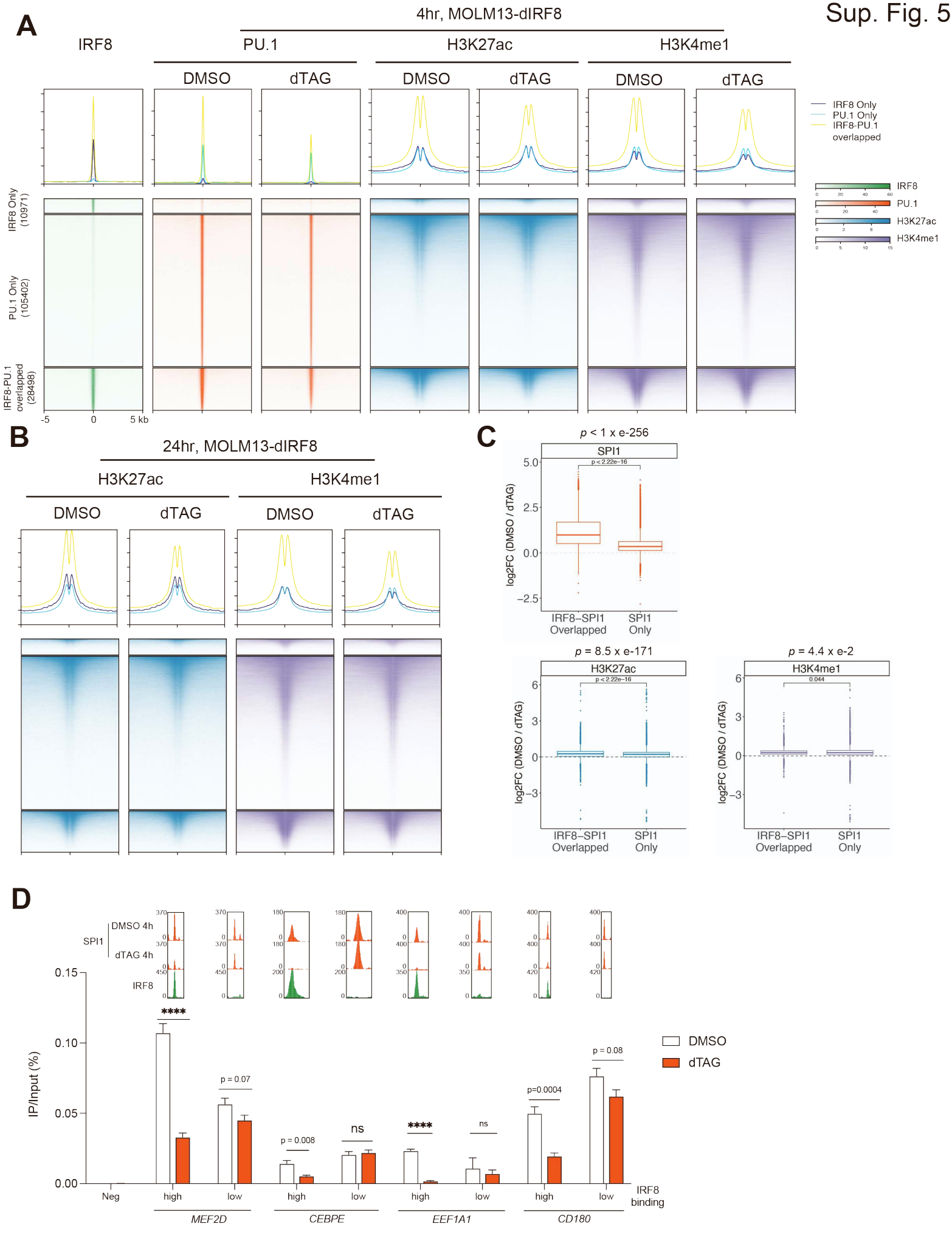
A
4hr, MOLM13-dIRF8
IRF8
PU.1
H3K27ac
H3K4me1
DMSO
dTAG
IRF8 Only
PU.1 Only
IRF8-PU.1 overlapped
IRF8 Only (10971)
PU.1 Only (105402)
IRF8-PU.1 overlapped (28498)
-5
0
5 kb
IRF8
PU.1
H3K27ac
H3K4me1
B
24hr, MOLM13-dIRF8
H3K27ac
H3K4me1
DMSO
dTAG
C
p < 1 x e-256
SPI1
p < 2.22e-16
log2FC (DMSO / dTAG)
IRF8–SPI1 Overlapped
SPI1 Only
p = 8.5 x e-171
H3K27ac
p = 4.4 x e-2
H3K4me1
0.044
D
SPI1
DMSO 4h
dTAG 4h
IRF8
IP/Input (%)
DMSO
dTAG
****
p = 0.07
p = 0.008
ns
****
ns
p=0.0004
p = 0.08
Neg
high
low
IRF8 binding
MEF2D
CEBPE
EEF1A1
CD180

Figure S5. IRF8 supports PU.1's chromatin occupancy and transcriptional output. Related to Figure 4.
(A-B) Metaplots and heatmaps of ChIP-seq with indicated cells in Figure 4c at IRF8-only, PU.1 only and IRF8-PU.1 overlapped regions (n=3) upon 4hr (A) or 24hr (B) dTAG treatment. (C) Boxplots depicting the log2FC of DMSO vs dTAG tag counts of ChIP-seq in K. Two-side Welch's t-tests were performed for statistical analysis. (D) ChIP-qPCR with PU.1 antibody at select IRF8-high or low/unbound elements in MOLM13-dIRF8 cells treated with DMSO or 500nM dTAG-47 (n = 4-5, mean ± SEM).

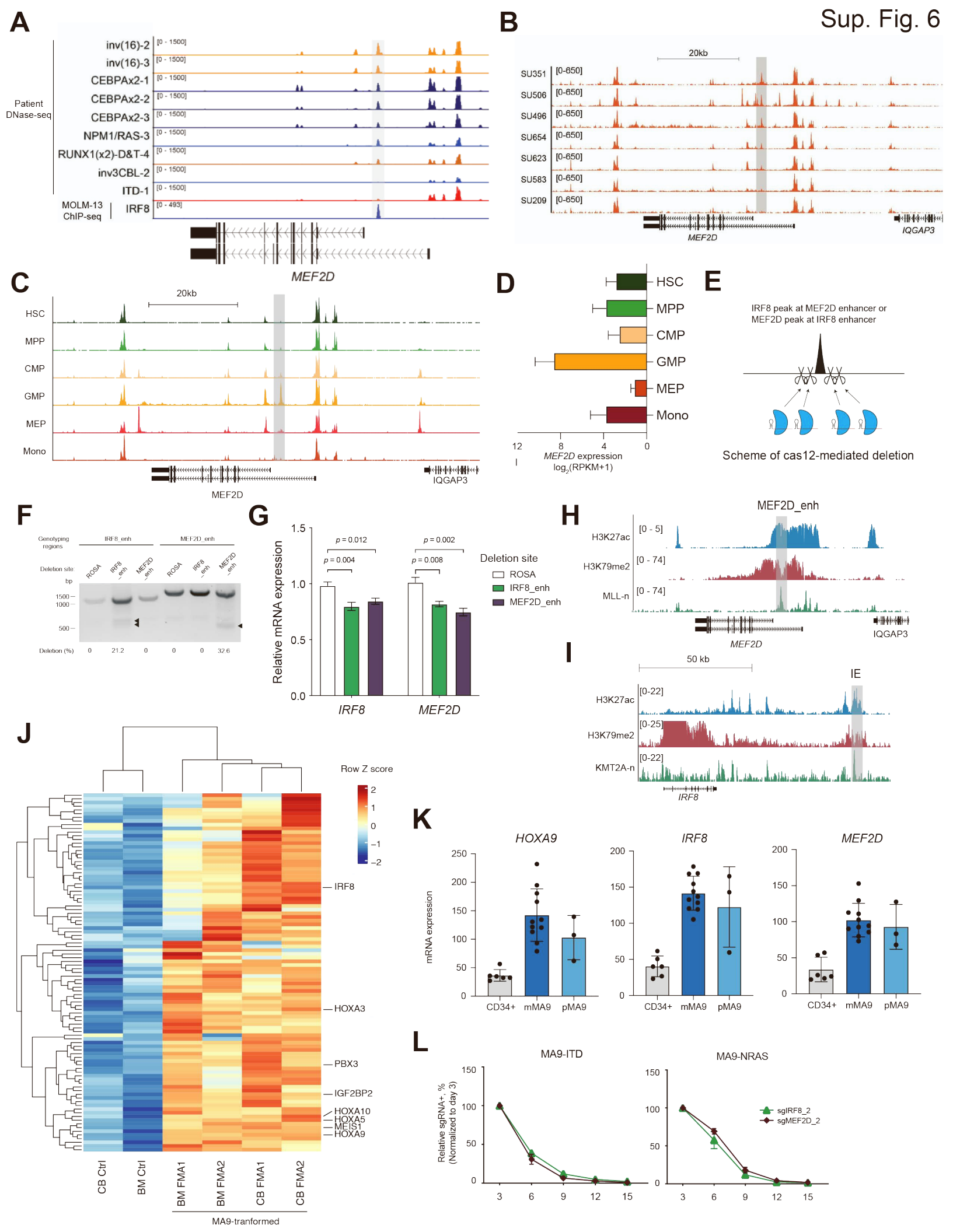
A
Patient DNase-seq
inv(16)-2
inv(16)-3
CEBPAx2-1
CEBPAx2-2
CEBPAx2-3
NPM1/RAS-3
RUNX1(x2)-D&T-4
inv3CBL-2
ITD-1
MOLM-13 ChIP-seq
IRF8
MEF2D
B
20kb
SU351
SU506
SU496
SU654
SU623
SU583
SU209
MEF2D
IQGAP3
C
20kb
HSC
MPP
CMP
GMP
MEP
Mono
MEF2D
IQGAP3
D
HSC
MPP
CMP
GMP
MEP
Mono
MEF2D expression log2(RPKM+1)
E
IRF8 peak at MEF2D enhancer or
MEF2D peak at IRF8 enhancer
Scheme of cas12-mediated deletion
F
Genotyping regions
IRF8_enh
MEF2D_enh
Deletion site
ROSA
IRF8_enh
MEF2D_enh
bp
1500
1000
500
Deletion (%)
0
21.2
0
0
0
32.6
G
Relative mRNA expression
p = 0.012
p = 0.004
p = 0.002
p = 0.008
Deletion site
ROSA
IRF8_enh
MEF2D_enh
IRF8
MEF2D
H
MEF2D_enh
H3K27ac
H3K79me2
MLL-n
MEF2D
IQGAP3
I
50 kb
IE
H3K27ac
H3K79me2
KMT2A-n
IRF8
J
Row Z score
IRF8
HOXA3
PBX3
IGF2BP2
HOXA10
HOXA5
MEIS1
HOXA9
CB Ctrl
BM Ctrl
BM FMA1
BM FMA2
CB FMA1
CB FMA2
MA9-tranformed
K
HOXA9
IRF8
MEF2D
mRNA expression
CD34+
mMA9
pMA9
L
MA9-ITD
MA9-NRAS
Relative sgRNA+, %
(Normalized to day 3)
sgIRF8_2
sgMEF2D_2

Figure S6. MEF2D and IRF8 are upregulated in AML carrying KMT2A-r through enhancer reactivation. Related to Figure 5.
(A) Gene tracks of DNase I-seq (Assi et al., 2019) signals in primary AML patients of indicated subtypes. MOLM-13 IRF8 ChIP-seq were from (Cao et al., 2021). (B) Gene tracks of ATAC-seq signals (Corces et al., 2016) in primary AML patients. (C) Gene tracks of ATAC-seq signals (Corces et al., 2016) in healthy donor hematopoietic cells in MEF2D locus. HSC, Hematopoietic stem cell; MPP, Multipotent progenitor; CMP, Common myeloid progenitor; GMP, Granulocyte monocyte progenitor; Mono, Monocyte; MEP, Megakaryocyte-erythroid progenitor. (D) Bar graph showing MEF2D mRNA expression in healthy donor hematopoietic cells. (E) Schematic of the crRNA design to conduct Cas12-mediated deletion of enhancers. (F) Genotyping and efficiency quantification of enhancer deletions in MOLM-13 cells on day 5 post-infection. ROSA serves as a negative control. Band intensities were normalized by product size. Percentage of anticipated enhancer deletion was calculated using normalized enhancer-deleted band (arrowhead) intensity divided by sum of normalized enhancer-deleted and intact band intensity. (G) RT-qPCR analysis of IRF8 and MEF2D after deletion of the IRF8 or MEF2D enhancer on day 5 post-infection (normalized to GAPDH, n=5-7, mean ± SEM, Student's t-test). (H-I) Gene tracks of ChIP/CUT&RUN signals (Krivtsov et al., 2019) of H3K27ac, H3K79me2 and KMT2A-n at MEF2D or IRF8 (D) locus in MOLM-13 cells. (J) Heatmap depicting upregulated genes in lentivirus-mediated MA9-transformed HSPCs from both BM and CB compared with healthy donor HSPCs isolated from BM and CB (Horton et al., 2013). BM, Bone marrow. CB, Cord blood. (K) Significantly upregulated gene (including HOXA9, IRF8, MEF2D) expression in retrovirus-mediated MA9-transformed human AML cells. mMA9, isolated human CD34+ HSPC were transformed with MA9, maintained in culture (~30 days), engrafted into mice, and AML blast cells were harvested from mice that developed leukemia (Barabé et al., 2017). pMA9, pediatric MA9+ AML samples. (L) Competition-based proliferation assays in MA9-FLT3ITD (left) or MA9-NRASG12D (right) cells with indicated sgRNAs (n=3, mean ± SEM).

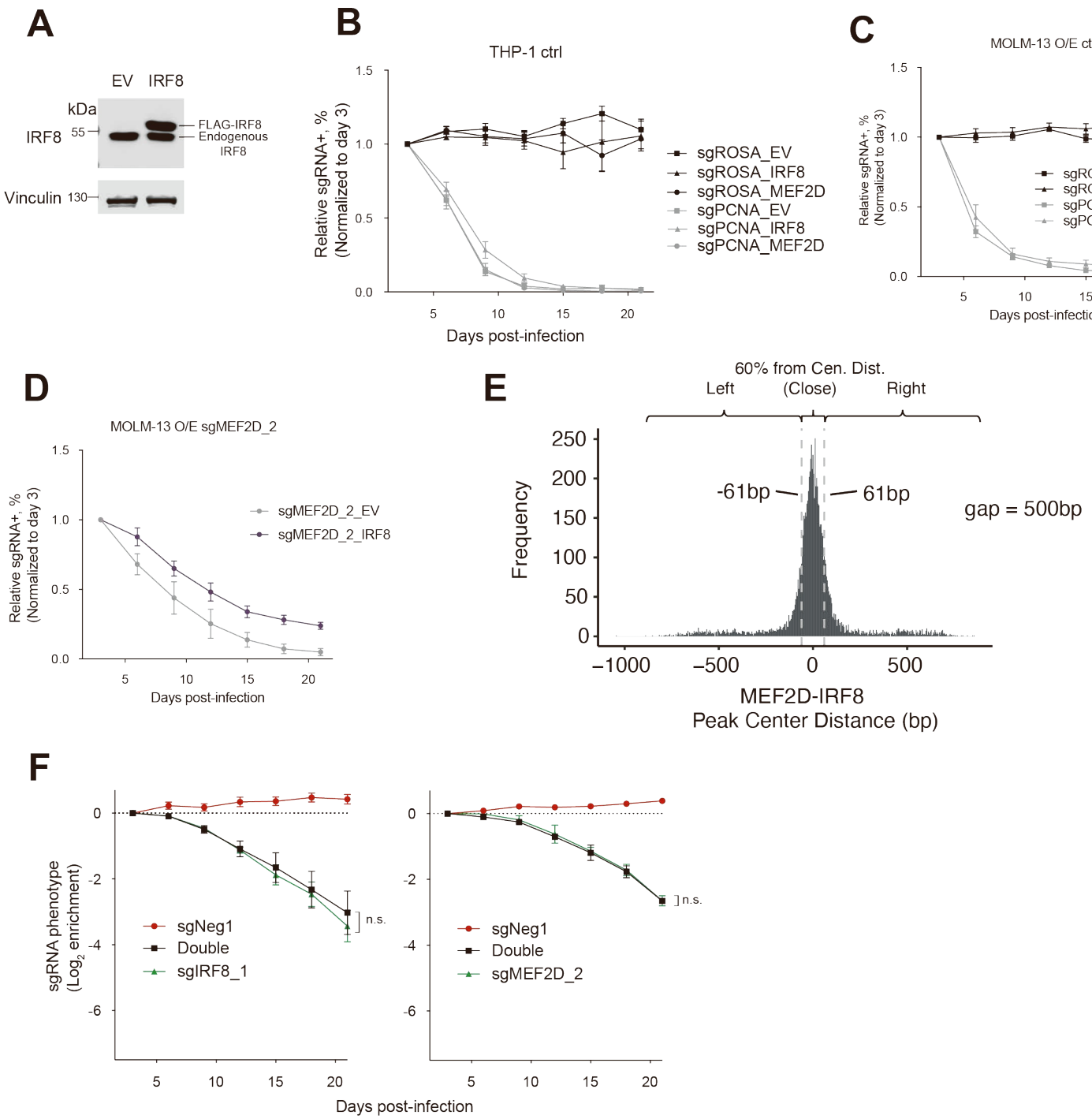

Figure S7. Divergent function of MEF2D- and IRF8- regulated programs in supporting AML. Related to Figure 6.
(A) Immunoblotting of endogenous IRF8 and FLAG-IRF8 in THP1 w le cell lysates with indicated vector expression. (B) Competition-based proliferation assays in THP-1 cells transduced with EV or indicated cDNA, and subsequently control sgRNA (n= 3-4, mean ± SEM). (C-D) Competition-based proliferation assays in MOLM-13 cells transduced with EV or IRF8 cDNA (Cao et al., 2021), and subsequently indicated sgRNA (n= 3-4, mean ± SEM). (E) Histogram depicting MEF2D-IRF8 peak distance distributions. A MEF2D-IRF8 peak pair will count if their distance is within 500bp (gap = 500). Distances that are the lowest 60% are considered "close", and the others are considered "left" or "right" depending on IRF8 location at upstream or downstream. (F) Competition-based proliferation assays in THP-1 cells simultaneously transduced with sgIRF8_1+ sgNeg1+ or sgMEF2D_2+sgNeg linked with GFP or mCherry. Uninfected cells serve as an internal control (n= 2-4, mean ± SEM. n.s, not significant, two-tailed Welch's unpaired t-test).

PU.1 signature

TASL	KIF20B	ZNF33A	DHX29	ANKRD12
MT-ATP8	ATAD5	RPS6KA4	MS4A7	PHF3
BEX1	GALNT6	KMT2A	ARID5B	COLGALT2
H4C3	AP1S3	CCDC88B	TTC32	E2F7
CADM1	MIS18BP1	PRIM1	ACVRL1	IL6R
VCAN	CENPQ	PSTPIP1	GOLGA2	RAB11FIP2
FYB1	SMC6	RPL41	ASH1L	ZFC3H1
H1-2	CEP83	ALCAM	KLHL8	DDX60
PSMC1	DDX59	IFT81	ARHGAP25	PEX1
MTRNR2L12	SIAE	FZD3	CSPP1	FNBP4
EIF4A1	ARL11	AKAP9	DYNC1I2	ZNF556
GNL3	LILRA2	GCC2	LTN1	UBR4
KMT5A	DAPP1	PRR14L	STOX2	ZNF526
GNL3L	TXLNG	DHX36	PRRC2C	CHORDC1
JRKL	ZC3H13	TMF1	THAP6	HRH2
ALG11	FAHD2A	CYBB	PARP4	PPP6R1
IL12RB1	SPTLC1	PHACTR2	SCAPER	NDE1
PDIA3	CEP290	ZFR	ITSN1	TLR2
ITGA4	PABPC3	ZNF480	ZGRF1	PPIB
FGL2	SRGAP2C	NSD1	PRKAR2B	CENPF
NCR3LG1	GIGYF2	DNAJC21	TGS1	MAP7D3
CDK11B	ZCCHC9	DDX60L	CCDC82	CLU
CD84	BOD1L1	ZNF714	PSPN	ATF5
COX16	FILIP1L	BST2	NSRP1	CEP89
TYROBP	REST	CCDC125	SCLT1	PCM1
ZNF675	KPNA3	CYP1B1	RBM47	NRDC
CIP2A	GAPT	USP16	UVSSA	RBBP5
TOP1	PTPN11	PRPF4B	CYP2S1	ZBTB7A
CNTRL	TPR	ZNF638	STAT3	NOXS
TFEC	CNTLN	ROCK2	CWC22	RFC3
ITGB1	FAM107B	KLF3	PTMA	FANCM
CLSPN	PURA	RSL1D1	PHF14	BTBD7
GOLGA4	LRRFIP1	OSBPL1A	SH3KBP1	ZNF440
SMC3	ESCO2	TOPORS	LY9	NUCKS1
TONSL	ZNF808	ARID4B	RINL	MRPS31
XRCC1	CUX2	ZNF280C	AIF1	STK36
BAX	ERC1	CASP8AP2	SMC2	FXR1
EIF3A	CEBPZ	ZMAT2	CEP104	UHRF1BP1L
BTK	MTHFR	CEP135	TNFSF14	PIGM
TNFSF10	MAP10	PPP1R10	KIAA0232	CARD6
SRRM1	VAC14	ARFGEF2	SIGLEC10	ST3GAL6
TEX15	RAD51AP1	PWWP2A	BTAF1	GNB4
SAMHD1	MTURN	TGM5	BICDL1	SPAG9
MT-ND6	TRIM38	DIAPH3	IRF5	CCR1
ITPR2	TCF4	MOB1B	MEX3A	PLCL2
CD36	REV3L	PCNT	SMC1A	RRP15
TMEM156	FGD2	GOLGA8N	MAML3	ATP6V1C2
PTPRC	AFF3	BPTF	SUDS3	RBL1
REL	SGK3	DBF4	TAF2	LARS1
ULBP4	POLR1G	GOLIM4	SLC39A10	GPR65
GPATCH11	PIBF1	SRSF11	ACOT11	PORCN
ACSM3	CEP295	TRAPPC10	NRGN	CCDC66
MT-ND5	DHTKD1	CRYBG3	PRRG4	DDX52
CPM	LGALS9	NOC3L	CORO2A	MT-ND2
ANO8	PUS7L	FAM43A	BRD4	PDCD7
EEA1	GON4L	RALBP1	WASL	CEP350
SPECC1	AGTPBP1	HGF	SMARCC1	MED25
MYO18A	ASPM	RAD50	NOP56	DBF4B
SBDS	KIF2A	ENC1	H2BC15	BMP4
SRFBP1	CMTM7	EIF4G3	TBC1D8	ABCF1
PTAFR	RBM25	GOLGB1	TENTSA	BZW1
MEGF8	BAZ2B	RESF1	DZIP3	ANKIB1
RBM41	HMGN2	TAF3	NKTR	CNNM2
BAZ1B	ZNF773	RPAP3	ZSWIM9	MYSM1
WDR70	GPATCH8	DDX10	TOGARAM1	SLC66A1
SERPINB8	LRRC69	ANKRD11	PAK1	CEP128
YBX1	INTS3	ZNF670	ATF7IP	MTRF1L
ATRIP	TMEM159	SLC12A5	LARP7	IFT74
ARL13B	PRPF38B	PDS5B	SBNO1	FAM13B
TRIP11	MYO5A	MS4A6A	KCNK6	LIMA1
LY2	ARHGAP26	ENDOD1	PKN2	TTF1
NLRC4	VIT	CD2AP	RBM4	ZNF430
XAF1	SUPT16H	LPAR6	OFD1	PRPF18
EEF1A1	FGD4	ESF1	TYW3	FAM20C
H2AC20	KIF3A	KRIT1	ADA2	HOOK3
HDAC7	ANKRD26	ELF1	CSNK1A1	BICD1
POU2F2	APOBR	TOP2A	CENPJ	DNAJC2
PRR11	PTK2B	FKBP8	SLC9A7	BICD2
IRAK4	GRN	PTPRE	FCGR1A	KIF15
BDP1	TCEA1	PDCL3	PIK3R5	AARSD1
TTI1	VHL	SHPRH	SEPTIN11	KTN1
CCDC18	DENND1C	MT-ND1	RAB29	MKI67
NFAT5	CCDC88A	PPIG	TMEM183A	NME2
MED24	SWAP70	NEXN	ITGB3BP	LRRCC1
CENPE	RB1CC1	AP2B1	SLC26A8	IFI6
CEP162	MTDH	ROCK1	RRBP1	ZNF836
TPM3	CLIP1	ABCF2	SERPINB10	ANKRD36C
DYNLT3	ORAI2	STIM2	HMOX1	BRCA2
ZNF346	POLD3	ALKBH4	PEAK3	AKAP8
ARID4A	CSF2RA	PGM2L1	MNS1	RSF1
CCDC186	RGS18	EP300	EPHB3	OSBPL8
PNOC	MS4A4A	GAS2L3	UTP23	APC
NCF2	LPAR4	IRF2	TRIM14	ZNF326
TM9SF1	MPHOSPH10	TBC1D32	SLTM	BUB1
LUZP1	NDUFS2	ALDH4A1	MSL3	CLINT1
ASRGL1	KIF16B	CHD1	RBBP6	PAK2
SLITRK4	HMGN5	SAFB2	ERCC6L2	RNASE3
		CCDC112	ESCO1	GPATCH4
		ZC3H18	TIFAB	LTV1
		JMJD1C	METTL2B	TLN1
				CHST2
				DTNA
				PHF20L1
				FAM135A
				ZNF106
				INHBA

Table S1. PU.1 signature used in this study. Related to Figure 4. Note: PU.1 signature was defined as top 500 downregulated genes upon CRISPR/Cas9-mediated PU.1 depletion in MOLM-13 cells.

sgRNA/crRNA Name	sgRNA/crRNA Sequence	Note
sgMEF2D_1	TCCAGCGAATCACCGACGAG	
sgMEF2D_2	ACTTTCACCAAGCGGAAGTT	
sgPU.1_1	GCTCCGCAGCGGCGACATGA	
sgPU.1_2	GCAGCGCGCGCGCCATCTTC	
sgMEF2D_enh_1	CTAATGGTTAGATCAGGGGA	
sgMEF2D_enh_2	ATGAGCCAATGGAGGCCTAG	
sgMEF2D_enh_3	TGCCCAAAAGACTTCAGGGT	
sgNeg	GAAGATGGGCGGGAGTCTTC	sgRNA targeting ROSA
sgNeg2	GGCCAGGCTTTGGGGAGGCC	sgRNA targeting neuronal gene *EMX1*
sgPCNA	GGACTCGTCCCACGTCTCTT	
sgIRF8_1	ATTGACAGTAGCATGTATCC	
sgIRF8_2	AGAGCATGTTCCGGATCCCT	
crROSA-1	CAACAATAGATGTATTGAGA	
crROSA-2	GGCCTATTCTCAGTCCAGGG	
crROSA-3	AGTGTCTATCACCTCTCCCG	
crROSA-4	TTGATCCTTTGCCTTGATCC	
crIRF8_1	TCTGATTCTGCCAAGTCCCC	
crIRF8_2	GCCCTATCGTACAGAGTCTG	
crIRF8_3	CCTGAGGCCACACAGTGATG	
crIRF8_4	TGCCAAGTTCCTCTCCTTCA	
crMEF2D_1	TCAGAAGCCCTCCAACCAAGCAT	
crMEF2D_2	GGGTCCCCTGTCATCATCGTAGG	
crMEF2D_3	CACCTCCCCTTTCCTCATAATTG	
crMEF2D_4	AGCCCCAGAGACTACTTTGAGTC	
sgNeg3	AATGGCAACTGGTCCCCTTC	sgRNA targeting murine *Ano9*
sgRpa3	ACGGGCCGGTCGATATACTG	
sgMef2d_1	GCACAGCACACTCAGCTCGT	
sgMef2d_2	GAGCAGCACCTTGTCCATGT	

Table S2. sgRNA/crRNA sequences. Related to Figure 2-5.

Primer name	Primer sequence	Usage	Note
GAPDH_F	CCTGACCTGCCGTCTAGAAA	RT-qPCR	
GAPDH_R	CTCCGACGCCTGCTTCAC	RT-qPCR	
MEF2D_all_F	atggggagagggtcttcagt	RT-qPCR	Primers to amplify the last exons of MEF2D that both isoforms contain (NM_005920 and NM_001271629)
MEF2D_all_R	cacagaccatcccagtgttg	RT-qPCR	
MEF2D_short_F	AGTTCTTAGGGTGCCTGGGG	RT-qPCR	Primers to detect the MEF2D short isoform
MEF2D_short_R	AGGATACCTTCGACTGGGGA	RT-qPCR	
MEF2D_long_F	GACAACACCGTTCCCCCAG	RT-qPCR	Primers to detect the MEF2D long isoform
MEF2D_long_R	GCTCATGAACGGTCTGGGAA	RT-qPCR	
ChIP_Neg_F	GGTCAGGCCAACTTGATTGT	ChIP-qPCR	hg19: Chr8: 129846262 -129846360
ChIP_Neg_R	AATTTGTGTTGGGCCACATT	ChIP-qPCR	
PU1_ChIP_1F	TGTGTCACCTTCCACCTCC	ChIP-qPCR	chr1:156462569-156462638, IRF8 high
PU1_ChIP_1R	GCTGCCACTTTCACTTCTGT	ChIP-qPCR	
PU1_ChIP_2F	TTGTATCTGGTGTGGGGTAGG	ChIP-qPCR	chr1:156493761-156493830, IRF8 low
PU1_ChIP_2R	TGGTGTCAGGACAACTGGAA	ChIP-qPCR	
PU1_ChIP_3F	AAGTGTGCCCTCTGGCTCT	ChIP-qPCR	chr14:23584348-23584418, IRF8 high
PU1_ChIP_3R	GCTGAACACATCCCAATCCT	ChIP-qPCR	
PU1_ChIP_4F	TCTGCTTCCTTTTCCTTCCTC	ChIP-qPCR	chr14:23588485-23588569, IRF8 low
PU1_ChIP_4R	CTCCCTGAGTCACCCCAAG	ChIP-qPCR	
PU1_ChIP_5F	TGCTAAAATGTGGCCTGTCA	ChIP-qPCR	chr6:74224970-74225067, IRF8 high
PU1_ChIP_5R	TGGGACACGATTTGTTCAGA	ChIP-qPCR	
PU1_ChIP_6F	GAAAAAGGCGGAGCCAGTA	ChIP-qPCR	chr6:74230806-74230876, IRF8 low
PU1_ChIP_6R	AACCGGTGCCTAGAGAAGGT	ChIP-qPCR	
PU1_ChIP_7F	AGCTGAAGGGGGAAGAAGAA	ChIP-qPCR	chr5:66489087-66489173 , IRF8 high
PU1_ChIP_7R	GGCCGTTTTTCAAGGGTAA	ChIP-qPCR	
PU1_ChIP_8F	GTGGCTCTGTGCTGGAAAA	ChIP-qPCR	chr5:66492618-66492711 , IRF8 low
PU1_ChIP_8R	GGGGTTGGGTCCTCAGTTAT	ChIP-qPCR	
IRF8_geno_F	CATGCCTGAACAAACCCACT	genotyping	
IRF8_geno_R	CCCTCATCTCCCCACACTAA		
MEF2D_geno_F	AAGGGGTGTGAAATCACGAG	genotyping	
MEF2D_geno_R	CTTTCCTGAAAGCAGCAAGC		
enIRF8_p2F2	TCAAAGAAGTGTTTTGCTTTCG	CUT&RUN-qPCR	chr16:86018660-86018735
enIRF8_p2R2	GAAGTGCCTATGCTGCCTTC		
enIRF8_p1F2	TGGCCATGTGTGTCTATGTG	CUT&RUN-qPCR	chr16:86016462-86016524
enIRF8_p1R2	CCACCCACTGACACGAGAG		

Table S3 qPCR/genotyping primer sequences. Related to Figure 2-5.

Collection ID	Sample Type	Collection Status	Diagnosis	Subtype	WBC	Gene	Categorization	tein Mutation T	Protein Change	NA Mutation Ty	cDNA Change	Variant Effect	Insertion Length	FAF %	Position	Exon
4943	Pheresis	De Novo	AML	AML with 11q23 abn	109.2	PHF6	Disease Associated	frameshift	p.M46Ifs*35	deletion	c.138delG	FRAME_SHIFT		96.12	133511785	
6315	Pheresis	De Novo	AML	AML with 11q23 abn	133.5	FLT3	Disease Associated	substitution	c.1352C>T	missense	p.S451F	missense_variant	1	22.97	28610138	11
						NRAS	Disease Associated	substitution	c.34G>T	missense	p.G12C	missense_variant	1	5.26	115258748	2
						NRAS	Disease Associated	substitution	c.182A>T	missense	p.Q61L	missense_variant	1	15.51	115256529	3
						STAG2	Disease Associated	duplication	c.1023_1024du	frameshift	p.E342Vfs*3	frameshift_variant	1	41.49	123184975	12

Table S4. clinical follow-up of AML patients used in this study. Related to Figure 5.

Name	Genetics	Subtype
MOLM-13	MLL-AF9/FLT3-ITD	AML
MOLM-14	MLL-AF9/FLT3-ITD	AML
MV4;11	MLL-AF4/FLT3-ITD	AML
NOMO-1	MLL-AF9/KRASG13D/TP53/EP300	AML
THP-1	MLL-AF9/NRASG12D/TP53	AML
OCI-AML3	DNMT3AR882C/NRASQ61L/NPM1mut	AML
ML-2	MLL-AF6/KRASA146V	AML
OCI-AML2	MLL-AF6	AML
MONOMAC1	MLL-AF9/FLT3V592A/RUNX1A107V/TP53	AML
OCI-AML5	ASXL1/RUNX1/TET2/EZH2	AML
U937	CALM-AF10/PTEN/TP53/JAK3M511I	AML
EOL1	KMT2A-amp	AML
HEL	JAK2V617F/TP53	AML
SET2	JAK2V617F/TP53/DNMT3AR882H	AML
P31/FUJ	KMT2Amut/NRASG12C/[TEN/RAD21H208R/TP53	AML
SHI1	MLL-AF6/KRASQ61H/TP53	AML
KASUMI1	AML1-ETO/KIT/RAD21/TP53	AML
OCIM2	RUNX1-TSPEAR/NRASQ61K/TP53	AML
HEL9217	JAK2V617F/TP53	AML
TF1	CBFA2T3-ABHD12/NRASQ61P/TP53	AML
F36P	KMT2Amut/TP53	AML
NB4	PML-RARA/KRASA18D/TP53	AML
AML193	NRASG13V/TP53	AML
M07E	ANO7-DHDH /CBFA2T3-GLIS2/NRASQ61K	AML
MUTZ8	JAK2V617F	AML
KO52	DNMT3AR882C/NRASG13R/TP53	AML
EM2	BCR-ABL1/TP53	CML
K562	BCR-ABL1/TP53	CML
KYO1	BCR-ABL1/TP53	CML
KU812	BCR-ABL1/TP53	CML
NCO2	BCR-ABL1/TP53	CML
KCL22	BCR-ABL1/TP53	CML
JURLMK1	BCR-ABL1/TP53/KMT2D	CML
JURKAT	TP53/NOTCHR1627H/FBXW7/BAX/MSH2/MSH6	T-ALL
PF382	TP53/NOTCH1	T-ALL
SUPT1	TP53/PIK3CA/KIT/EGFR	T-ALL
HSB2	NOTCH1L1600P//NRASG12C/TP53.PIK3R1.FGFR3/ERBB2	T-ALL
NALM16	NOTCHD1698N	B-ALL
HB1119	TP53/MLL-ENL	B-ALL
SEMK2	MLL-AF4/CDKN2A/TP53	B-ALL
JM1	BCL2/KMT2D	B-ALL
ROS50	BCL2/BCL3/TP53	B-ALL
P30OHK	ASXL1/ASXL3/BCL9/KMT2Amut/KMT2D	B-ALL
697	TCF3-PBX1/	B-ALL
SEM	MLL-AF4/CDKN2A/TP53	B-ALL
NALM6	EGFR/NRASA146T/RARA	B-ALL
CII	Unspecified	B-cell non-specified
HG3	KMT2B/KMT2D/RARA	B-cell non-specified
PGA1	KRASA146V/XPO1	B-cell CLL
MEC1	R3HCC1L-HTRA1/TP53	B-cell CLL
CI	Unspecified	B-cell CLL
REH	TEL1-RUNX1	B-ALL

Table S5. Leukemia cell line information. Related to Figure 1.

Sample Name	% Dups	% GC	M Seqs
MOLM13_dIRF8_4h_DMSO_H3K27ac_rep2_S1_R1_001	18.90%	46%	18.6
MOLM13_dIRF8_4h_DMSO_H3K27ac_rep3_S5_R1_001	28.10%	46%	19.9
MOLM13_dIRF8_4h_DMSO_H3K4me1_rep2_S2_R1_001	11.40%	43%	19.7
MOLM13_dIRF8_4h_DMSO_H3K4me1_rep3_S6_R1_001	18.00%	42%	19.7
MOLM13_dIRF8_4h_DMSO_PU1_rep2_S13_R1_001	20.80%	40%	21.7
MOLM13_dIRF8_4h_DMSO_PU1_rep3_S14_R1_001	26.10%	41%	20.5
MOLM13_dIRF8_4h_DMSO_input_rep3_S11_R1_001	7.40%	38%	19.5
MOLM13_dIRF8_4h_dTAG_H3K27ac_rep2_S3_R1_001	18.40%	46%	22.2
MOLM13_dIRF8_4h_dTAG_H3K27ac_rep3_S7_R1_001	19.30%	46%	21.1
MOLM13_dIRF8_4h_dTAG_H3K4me1_rep2_S4_R1_001	12.00%	42%	23.4
MOLM13_dIRF8_4h_dTAG_H3K4me1_rep3_S8_R1_001	13.70%	42%	19.3
MOLM13_dIRF8_4h_dTAG_PU1_rep2_S15_R1_001	25.50%	40%	20.7
MOLM13_dIRF8_4h_dTAG_PU1_rep3_S16_R1_001	21.20%	41%	18.5
MOLM13_dIRF8_4h_dTAG_input_rep3_S12_R1_001	8.00%	38%	21.5
MOLM13_dIRF8_DMSO_4h_input_rep2_S9_R1_001	6.10%	38%	20.7
MOLM13_dIRF8_dTAG_4h_input_rep2_S10_R1_001	5.30%	38%	19
MOLM13_dl8_24hr_DMSO_H3K27ac_S2_R1_001	5.00%	48%	16.5
MOLM13_dl8_24hr_DMSO_H3K4me1_S1_R1_001	3.40%	42%	19.9
MOLM13_dl8_24hr_DMSO_input_S9_R1_001	4.30%	38%	21.5
MOLM13_dl8_24hr_dTAG_H3K27ac_S4_R1_001	6.30%	46%	21.7
MOLM13_dl8_24hr_dTAG_H3K4me1_S3_R1_001	3.80%	42%	15.2
MOLM13_dl8_24hr_dTAG_input_S10_R1_001	3.60%	37%	20.1
MOLM13_dl8_4hr_DMSO_H3K27ac_S17_R1_001	7.70%	44%	22.5
MOLM13_dl8_4hr_DMSO_H3K4me1_S16_R1_001	5.60%	41%	21.2
MOLM13_dl8_4hr_DMSO_SPI1_S18_R1_001	23.10%	40%	31.6
MOLM13_dl8_4hr_DMSO_input_S22_R1_001	4.20%	38%	24.9
MOLM13_dl8_4hr_DMSO_old_H3K4me1_S15_R1_001	2.10%	41%	14.8
MOLM13_dl8_4hr_dTAG_H3K27ac_S20_R1_001	7.60%	48%	27.5
MOLM13_dl8_4hr_dTAG_H3K4me1_S19_R1_001	4.40%	43%	45.8
MOLM13_dl8_4hr_dTAG_SPI1_S21_R1_001	9.30%	38%	35.2
MOLM13_dl8_4hr_dTAG_input_S23_R1_001	5.10%	37%	21.9
MOLM13_abMEF2D_sgROSA_S2_R1_001	32.40%	43%	26.3
MOLM13_abMEF2D_zd370_S3_R1_001	11.10%	40%	22.6
p592_RNAseq_rep1_S30_R1_001	25.30%	46%	28.9
p592_RNAseq_rep2_S31_R1_001	26.90%	46%	44.2
p592_RNAseq_rep3_S32_R1_001	22.50%	45%	30.3
p6315_RNAseq_S20_R1_001	47.40%	48%	53.6
p6315_H3K27ac_S15_R1_001	27.80%	41%	27.9
p6315_IgG_R2_001	12.38%	40%	26.7
p592_IgG_S3_R1_001	13.00%	43%	11.8
p592_H3K27ac_S4_R1_001	19.40%	44%	18.8
MOLM13-MEF2D_CnR_R1	38.00%	41%	30.3

RNA-seq sample names	raw reads	Reads for mapping	Uniquely mapped %	Detected genes
MOLM13_sgPU.1_1	9117166	9096042	84.26	16861
MOLM13_sgPU.1_2	6,867,041	6,843,441	83.82	16,126
MV4-11_sgNeg_1	6,621,709	6,541,535	79.53	18,004
MV4-11_sgNeg_2	10,716,591	10,534,472	83.14	18,771
MV4-11_sgMEF2D_1	6,585,449	6,515,395	84.93	18,552
MV4-11_sgMEF2D_2	10,826,709	10,698,745	84.17	18,906
THP1_sgNeg_1	8,938,746	8,879,572	87.27	19,890
THP1_sgNeg_2	9,706,061	9,418,568	84.66	19,674
THP1_sgMEF2D_2_1	7,606,948	7,504,885	85.38	19,712
THP1_sgMEF2D_2_2	9,667,084	9,526,538	85.48	19,743
K562_sgNeg_1_1	6,547,677	6,465,326	85.89	17,191
K562_sgNeg_1_2	9,717,573	9,622,461	85.85	18,157
K562_sgMEF2D_1	9,358,548	9,244,481	86.08	18,328
K562_sgMEF2D_2	8,913,217	8,789,998	85.89	18,175

Table S6. Sequencing data information. Related to Figure 3-4.